An Improved Iris Localization Method

Meisen Pan
College of Computer and Electrical Engineering, Hunan
University of Arts and Science, China
pmsjjj@126.com

Qi Xiong
Hunan Province Cooperative Innovation Center for the
Construction and Development of Dongting Lake Ecological
Economic Zone, China
xiongqi@huas.edu.cn

Abstract: *Iris research has become an inevitable trend in the application of identity recognition due to its uniqueness, stability, non-aggression and other advantages. In this paper, an improved iris localization method is presented. When the iris inner boundary is located, a method for extracting the iris inner boundary based on morphology operations with multi-structural elements is proposed. Firstly, the iris image is pre-processed, and then the circular connected region in the pre-processed image is determined, the parameters of the circular connected region is extracted, finally the center and the radius of the circular connected region is obtained, i.e., the iris inner boundary is excavated. When the iris outer boundary is located, a method for locating iris outer boundary based on annular region and improved Hough transform is proposed. The iris image is first filtered, and then the filtered image is reduced and an annular region is intercepted, finally Hough transform is used to search the circle within the annular region, i.e., the center and the radius of the iris outer boundary is obtained. The experimental results show that the location accuracy rate of this proposed method is at least 95% and the average running time is increased by 46.2% even higher. Therefore, this proposed method has the advantages of high speed, high accuracy, strong robustness and practicability.*

Keywords: *Iris location, image pre-process, multi-structural elements, hough transform.*

1. Introduction

Iris is the annular region between the pupil and the sclera, which covers rich texture information. As an important biological feature of human body, iris research has become an inevitable trend in the application of identity recognition due to its uniqueness, stability, non-aggression and other advantages [2, 8, 11]. Iris location, as a crucial part of iris recognition, denotes that the iris region is separated from the iris image, and then the pupil, the sclera and other non-iris information existing in the iris image are eliminated. Therefore, iris location occupies a very important position in iris recognition and is also the premise and guarantee of subsequent processes, whose accuracy will directly influence the final iris recognition result. For a long time, the researchers around the world have reckoned it as the focus and difficulty of the preprocessing link, with significant theoretical and application value.

Since the iris inner and outer boundaries are approximately circular, essentially, iris location is to explore the center and the radius of the iris inner and outer boundaries. Generally, iris location is divided into two steps: the iris inner boundary location and iris outer boundary location. The iris inner boundary is the dividing line between the iris and the pupil, and the iris outer boundary one between the iris and the sclera. Therefore, the location of the iris inner boundary is essentially the segmentation of the pupil, which means that the acquisition of the iris inner boundary is that of the pupil boundary. In addition, there are certain constraints on the positions and radiuses between the iris inner and outer boundaries [1, 14]. For example, the coordinates of the center of the iris outer boundary are very close to those of the iris inner boundary, and the radius of the iris outer boundary is generally larger than but less than 3 times that of the iris inner boundary, which is conducive to locating the iris outer boundary.

The following sections in this paper are arranged as follows: section 2 introduces a brief literature survey on the related works. Section 3 elaborates the basic definitions and principles. Section 4 explains the location of the iris inner boundary. Section 5 presents the location of the iris outer boundary. Section 6 provides the experiments discussions. In the end, the conclusions are presented in section 7.

2. Related Works

In general, conventional iris location algorithms are divided into the following two categories: the method based on differential integral and, the method based on Canny operator and Hough transform. The first method believes that the iris is an approximate annular region, so iris location is simplified to refine the approximate center and the radius of the iris inner and outer boundaries. Daugman [6, 7] used integral-differential operator to detect circular parameters to

gradually obtain the iris inner and outer edges. This method requires traversing and searching all the parameter spaces, as a result, the algorithm complexity is relatively high. In order to improve the efficiency of this method, Zheng *et al*. [18] adopted integral operator combined with the expansion and contraction model to locate the iris in 2005. Schuckers *et al*. [15] pioneered elliptic integral operator combined with angle deformation model to position the iris. As the second method, Canny operator and Hough transform are commonly used for iris location. Boles [3] first introduced the edge detection operator to detect the edge points of the iris image, and then applied Hough transform to explore the parameters of the iris boundaries. Later, Bowyer *et al*. [4], Ma *et al*. [14], Sudha *et al*. [16] operated Canny operator and Hough transform to locate the iris. Tan *et al*. [17] divided the iris image into several different areas by using the change of gray value, located the pupil respectively by using difference integral, detected the eyelid by using the jump of gray value of shape and boundary pixel points, explored the eyelashes by using static statistical probability density function, and extracted the iris inner and outer boundaries by using Canny operator. Li *et al*. [12] used K-means clustering and improved Hough transform to position the iris. Chang *et al.* [5] proposed a novel iris segmentation technique based on active contour. This approach uses innovative algorithms, including two important ones, pupil segmentation and iris circle calculation. With their algorithms, the center position and radius of pupil is correctly found and the iris is precisely segmented. Lin *et al*. [13] proposed a Haar-like-feature-based iris localization method to quickly detect the location of human iris in the images captured by low-cost cameras for the ease of post-processing stages. The AdaBoost algorithm was chosen as a learning method for training a cascade classifier using Haar-like features, which was then utilized to detect the iris position. The experimental results have shown acceptable accuracy and processing speed for this novel cascade classifier. Efimov *et al*. [9] proposed a method for finding the iris area by approximating its boundaries by two circles. The relative error of determining the circle parameters must not exceed 5%. Convolutional neural networks optimized with respect to the number of parameters are applied. Jan *et al*. [10] proposed a robust iris localization scheme maintaining both speed and accuracy. It includes preprocessing the input eye image using an order statistic-filter and the bilinear interpolation scheme, extracting an adaptive threshold using the image's histogram, processing binary image via the morphological operators, extracting pupil's center and radius based on the centroid and geometry concepts, marking iris outer boundary using the Circular Hough Transform (CHT) and refining coarse iris boundaries through the Fourier series.

In this paper, on the basis of the analysis of Canny operator and Hough transform, we proposes an Improved Iris Localization Method (IILM). When locating the iris inner boundary, a method for extracting the iris Inner Boundary based on morphology operations with Multi-structural Elements (IBME) is explained and the general flow chart is listed in Figure 1. When locating the iris outer boundary, a method for locating iris Outer Boundary based on Annular region and Hough transform (OBAH) is introduced and the general flow chart is listed in Figure 2.
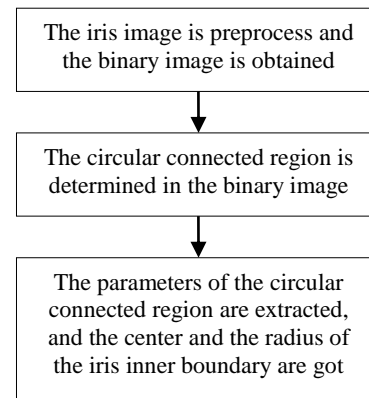
Figure 1. The flow chart of IBME.
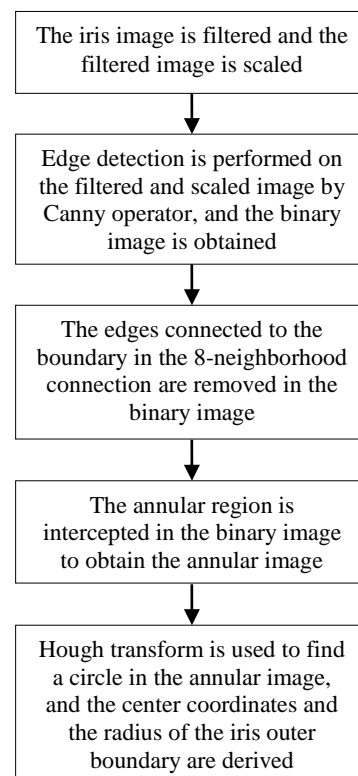
Figure 2. The flow chart of OBAH.

3. Basic Definitions and Principles

3.1. Region Features

- *Definition* 1. Assume that S denotes the connected region and B is the boundary of the region S. Then the region area A is expressed as follows:

$$P = \sum_{(x,y) \in B} (x, y) \tag{1}$$

Namely, circumference P is the number of pixels in the boundary B. The region area A is defined as follows:

$$A = \sum_{(x,y) \in S} (x, y) \tag{2}$$

Namely, A is the number of pixels in the region S, including B.

- *Definition* 2. The area A_{MER} of Minimum Enclosing Rectangle (MER) of the object in the image is defined:

$$A_{MER} = Ma \times Mi \tag{3}$$

Ma is the major axis and Mi is the minor axis of MER. Also, the aspect ratio Fc related to object shape is expressed:

$$Fc = \frac{Ma}{Mi} \tag{4}$$

Fc is the ratio of the width to the length of MER, which can distinguish a slender object from a circle or square object.

- *Definition* 3. Rectangle degree Rc is the ratio of the object area A to the area A_{MER} of the object MER, namely:

$$Rc = \frac{A}{A_{MER}} \tag{5}$$

Where $Rc \in [0,1]$. Especially, when the object is a circle or ellipse, $Rc = \pi/4 \approx 0.785$.

- *Definition* 4. Circularity degree Ci is the ratio of the square of the object circumference P to the object area A, namely:

$$Ci = \frac{P^2}{4\pi \times A} \tag{6}$$

Circularity degree ci reflects the complexity degree of the object boundary. More generally, the lower the value Ci is, the more irregular the object is, and the bigger the gap with the circle is. Instead, with a higher value Ci, the object is more regular and closer to the circle. From Equation (6), the circularity degree of a circle is $Ci = 1.0$.

3.2. K-means Clustering

In 1967, MacQueen proposed an unsupervised clustering algorithm, which is so-called K-means clustering algorithm. Since the algorithm classifies the data into a given number of clusters by minimizing the error function, it has simple principle and is easy to deal with large amounts of data. However, it must specify the number of clusters and iterations, or convergence condition, and the initial clustering center in advance. And then according to certain similarity criterion, each

sample data is assigned to the nearest or "most similar" clustering center to form a class. Finally by referring to the average vector of each class as the clustering center, each sample data is redistributed, and the clustering process iterates until the class converges or reaches the maximum number of iterations.

Suppose that $X=\{x_1,x_2,...,x_n\}$ expresses a set with n samples for $x_i=[x_{i,1},x_{i,2},..., x_{i,1}]^T(i=1,2,...,n)$, c is the given number of clusters, $V=\{v_1,v_2,...,v_c\}$ is a clustering center set with the element number c for $v_j=[v_{j,1},v_{j,2},..., v_{j,1}]^T(j=1,2,...,c)$, r_j denotes the sample number of each clustering set, and x_k^j is the kth sample belonging to the jth class. Then we define each clustering center by the following expressions:

$$v_j = \frac{1}{r_j} \sum_{k=1}^{r_j} x_k^j \qquad (x_k^j \in X) \tag{7}$$

So the objective function is defined as follows:

$$J(X,V) = \sum_{j=1}^{c} \sum_{k=1}^{r_j} d(x_k^j, v_j) \tag{8}$$

Where $d(x_k^j, v_j)$ is the distance between the sample x_k^j and its corresponding clustering center vj. The purpose of K-means clustering is to obtain the minimum of the above objection function. When K-means clustering, Euclidean distance is generally chosen as the distance $d(x_k^j, v_j)$, i.e., $d(x_k^j, v_j) = \left\| x_k^j - v_j \right\|^2$.

K-means clustering needs to set the clustering number c and the initial clustering center in advance, and it is sensitive to the initial clustering center. If the initial clustering center is well set, the convergence time of the algorithm can be effectively shortened. In this paper, Iterative Threshold Method (ITM), inspired by the idea of approximation, is used to generate the initial clustering center, which is depicted as follows:

- *Step* 1. An initial threshold value T is selected;
- *Step* 2. The image is divided into and two sets G_1 and G_2: $G_1 = \{I(x,y) \mid I(x,y) \leq T\}$ and $G_2 = \{I(x,y) \mid I(x,y) > T\}$, and then the mean gray values μ_1 and μ_2 of G_1 and G_2 are calculated respectively.
- *Step* 3. The new threshold $T' = (\mu_1 + \mu_2)/2$ is computed;
- *Step* 4. If $|T'-T| \leq \zeta$ (where ζ is a very small positive number specified in advance), i.e., if the thresholds obtained twice as before and after the iterations are close to each other, and then the iteration process terminates. Otherwise, let $T = T'$, and Steps 2-3 are repeated. So the last one T' is the threshold we need.

The purpose of setting the constant ζ is to finish the

algorithm as soon as possible and reduce the number of iterations. If the number of iterations is not concerned, it can be set to 0. In this paper, we have $\zeta = 0.5$ and take the average gray value of the image as the initial threshold T. Firstly, ITM is performed on all the gray values of the image to obtain the intermediate threshold T_0, then all the gray values of the image are divided into two sets I_1 and I_2 by T_0, i.e., $I_1 = \{I(x,y) \mid I(x,y) \leq T_0\}$ and $I_2 = \{I(x,y) \mid I(x,y) > T_0\}$, finally ITM is exerted on I_1 and I_2 to get the first and the second thresholds T_1 and T_2 respectively, which $[T_1 \ T_0 \ T_2]$ forms the initial clustering center of K-means.

In this paper, the iris image I is of $M \times N$ pixels with the upper left pixel being (1,1) and the gray level being L, the gray value at point (x,y) is $I(x,y)$. We use K-means clustering to cluster all the gray values of I. Before clustering, all the gray values of I are converted into a one-dimensional matrix, which are sorted in ascending order to form the sample set X with $k=1$. Moreover, ITM is employed o generate the initial clustering center of K-means, and X is divided into three classes by K-means clustering, finally three classes are sorted in ascending order. In conclusion, Gray clustering Method of the iris image Based on K-Means (GMKM) is explained as follows:

- *Step* 1. To further shorten the clustering time, the iris image I is reduced to 1/4, and the reduced I' is produced;
- *Step* 2. For I', all the gray values are converted into a one-dimensional matrix M in rows, sorted in ascending order;
- *Step* 3. According to M, ITM is used to generate the intermediate threshold T_0;
- *Step* 4. According to T_0, M is divided into two sets I_1 and I_2, i.e., $I_1 = \{I(x,y) \mid I(x,y) \leq T_0\}$ and $I_2 = \{I(x,y) \mid I(x,y) > T_0\}$, and the first threshold T_1 and the second threshold T_2 are obtained by ITM;
- *Step* 5. $[T_1 \ T_0 \ T_2]$ is taken as the initial clustering center of K-means;
- *Step* 6. M is grouped into three classes by K-means clustering;
- *Step* 7. The three classes $C_j(j=1, 2, 3)$ are sorted in ascending order, where C_1 is the smallest.

4. Location of the Iris Inner Boundary

On account of the relatively low pixel gray values in the pupil area, there are obviously difference between the pupil area and other ones in the iris image, which contributes to more easily segmentation of the pupil. In this paper, we propose a method for extracting the iris Inner Boundary based on mathematical morphology operations with Multi-structural Elements. First, the iris image is pre-processed, then the circular connected region is extracted, and finally the parameters of the circular connected region are derived, namely the iris inner boundary is obtained.

4.1. Preprocess of the Iris Image

The effective region of the iris is the approximately annular part between the pupil and the sclera, so iris location and separation are built on the pixel gray distributions of the iris, the pupil and the sclera. In the iris image, in general, common sense is that the pupil area is black, the iris is between black and gray, and the sclera is light gray. Also, there are a variety of noise information such as eyelids and eyelashes in the iris image, which must be filtered out to a certain extent when locating the iris. Generally, the image is preprocessed to remove noise interference. In this paper, we preprocess the iris image by the gray stretch transform.

In general, the gray values of the pupil are the lowest, those of the iris next, those of the sclera are the largest. However, so far it is difficult to separate the pupil, the iris and the sclera automatically and rationally. When preprocessing the iris image by the gray stretch transform, three gray values are obtained through K-means clustering combined with ITM, where the smallest, the middle and the maximum clustering values correspond to the average gray values of the pupil, the iris and the sclera regions respectively. Due to the low average gray value, in order to correctly explore the pupil, its gray values must be stretched. In order to dilute the noise information such as eyelashes, a series of mathematical morphology operations should be performed on the stretched image to obtain some connected regions. To facilitate the discussion and description, we define the image preprocessing function $[D, m]$=PrepImage($I, Area$), which is described as follows:

- *Function* 1. $[D, m]$=PrepImage($I, Area$)
- *Input parameters*: I is the gray iris image, and all the connected regions whose areas are less than $Area$ in the binary image are removed.
- *Output parameters*: D is the binary image produced by pre-processing the image I, and m is the initial size of the disk structural element Sel in section 3.2.
- *Step* 1. Initialization: *thresh* is the coefficient of variation, which reflects the degree of dispersion on the unit mean, and let *thresh*=0.4. Also, the disk structural element Se is the size of 2;
- *Step* 2. The gray Mean and standard deviation Std of the iris image I are calculated respectively:

$$Mean = \frac{1}{MN} \sum_{x=1}^{M} \sum_{y=1}^{N} I(x,y) \tag{9}$$

$$Std = \sqrt{\frac{1}{MN} \sum_{x=1}^{M} \sum_{y=1}^{N} [I(x,y) - Mean]^2} \tag{10}$$

- *Step* 3. The stretch threshold T_s is defined:

$$T_s = \max(\frac{Std}{0.4}, 150) \qquad (11)$$

Namely, we select the greater of $\frac{Std}{thresh}$ and 150 as T.

- *Step* 4. GMKM is used to cluster the gray values of I to obtain the smallest clustering value as the average gray value of the pupil.
- *Step* 5. If $Mean > T$, then

a) According to the following equation, the gray range of the iris image is stretched from $[0, C_1]$ to $[150, 255]$

$$G(x, y) = \begin{cases} \frac{255 - 150}{C_1} \bullet I(x, y) & 0 \le I(x, y) < C_1 \\ I(x, y) & I(x, y) \ge C_1 \end{cases} \qquad (12)$$

b) $m=5$.
c) In order to dilute the noise information such as eyelashes, the disk structural element Se is used to perform successively close and open operations on the stretched image G to obtain the image C, and go to Step 6.

Otherwise (i.e., $Mean \le T$),

a) The gray range of the iris image is stretched from $[0, 0.5C1]$ to $[150, 255]$, namely

$$G(x, y) = \begin{cases} 3.5 \bullet \frac{255 - 150}{C_1 + Std} \bullet I(x, y) & 0 \le I(x, y) < \frac{C_1 + Std}{3.5} \\ I(x, y) & I(x, y) \ge \frac{C_1 + Std}{3.5} \end{cases} \qquad (13)$$

b) $m=10$.
c) In order to dilute the noise information such as eyelashes, the disk structural element Se is used to perform successively open and close operations on the stretched image G to obtain the image C, and go to Step 6.

- *Step* 6. Sobel operator is adopted to detect the edges of C, and the edge image E is obtained.
- *Step* 7. The connected regions linking the boundary of the image E are removed in the 8-neighborhood connection, at the same time those whose area are less than $Area$ in the image E are also deleted, the pre-processed image D is produced, and the function ends.

4.2. Determining the Circular Connected Region

After the iris image is preprocessed, the preprocessed image D contains many areas with different sizes and shapes. Since the iris inner boundary is approximately circular, we need to explore an approximately circular region in D. Given all this, a method for Determining the Circular connected Region based on Geometric Features (DCGF) is put forward. DCGF takes the disk structural elements with different sizes to obtain the binary image D by the morphology close and open operations, uses the 8-neighborhood connection to find the connected region S_0 with the largest area in D_o, and determines whether S_0 is a circular connected region. When performing the close and open operations, the sizes of their disk structural elements are ascertained by cyclic variables. When judging the circular connected region, we calculate the geometric features of the connected region S_0 with the largest area: the area A, the ratio of the width and length Fc, the rectangle degree Rc, and the circularity degree Ci. In a number of experiments, we find that, as a connected region, if it satisfies all the following conditions: A>2000, $Fc \in [0.80, 1.15]$, $Rc \in [0.70, 0.8635]$ and $Ci \in [0.85, 1.25]$, then it is judged as a circular connected region. In order to determine whether there is a circular connected region in the binary image D_o, we define a marker $Mark$, where $Mark=1$ indicates that there is a connected region in D_o that meets the above circular judgment conditions, and $Mark=2$ denotes that there is no connected region in D_0 that conforms to the above circular judgment conditions. In order to facilitate discussion and description, we define the function $[D_0, Mark] = DCGF(D)$ of determining the circular connected region, which is described as follows:

- *Function* 2. $[D_0, Mark] = DCGF(D)$
- *Input parameters*: D is the preprocessed image;
- *Output parameters*: D_0 is the image produced by the function, and $Mark$ is the maker of the connected region in D_0 that meets the criterion of the circle determination.
- *Step* 1. *Initialization:* The array kk saves the serial number of the circular region detected in all the connected regions in the binary image, and $kk = []$. m is the size of the disk structural element $Se1$ belonging to the close operation, and its initial value is obtained by the image pre-processing function PreImage $(I, Area)$. n is the size of the disk structural element $Se2$ belonging to the open operation. D' is the pre-processed image and let $D' = D$. C_i and R_i are the center and the radius of the iris inner boundary respectively
- *Step* 2. If all the pixel values in D are 0, then go to Step 13; Otherwise, go to Step 3 and continue.
- *Step* 3. If $kk = []$ and $m \le 20$, then run Step 4-step 12; Otherwise, go to Step 13.
- *Step* 4. let $D = D'$ and $n=5$.
- *Step* 5. The binary image D_c is obtained by performing the close operation with the structural element $Se1$ with the size of m on D.
- *Step* 6. The hole regions are filled in D_c and the binary image D_i is produced;
- *Step* 7. If $kk = []$ and $n \le 40$, then run Step 8-Step 11; Otherwise, go to Step 12.

- *Step* 8. The binary image D_o is obtained by performing the open operation with the structural element *Se2* with the size of n on D.
- *Step* 9. The connected region S_0 with the largest area in D_o is searched in the 8-neighborhood connection, and i is the number of S_0.
- *Step* 10. For S_0, the following geometrical features are computed:

  a) The area A of the connected region is calculated according to Equation (2).
  b) The ratio of the width and length Fc is worked out according to Equation (4).
  c) The rectangle degree Rc is solved according to Equation (5).
  d) The circularity degree Ci is counted according to Equation (6).
  e) If the geometrical features of S_0 satisfy simultaneously: $A>2000$, $0.70 \le Rc \le 0.8635$, $0.85 \le Ci \le 1.25$, and $0.80 \le Fc \le 1.15$, then S_0 is a circular connected region, and we have $kk = [i]$;

- *Step* 11. Let $n = n+5$, go to Step 7 and continue.
- *Step* 12. Let $m = m+5$, go to Step 3 and continue.
- *Step* 13. If $kk <> []$, then *Mark*=1; Otherwise, *Mark*=2 and D_0=D.
- *Step* 14. Return D_0 and *Mark*, and the function ends.

4.3. Extraction of the Parameters of the Connected Region

After the circular connected region is determined, the image D_o is processed differently according to *Mark*. If *Mark*=1, means that only 1 circular connected region is retained in D_o, and the parameters of the iris inner boundary can be obtained by calculating the center and the radius of the circular connected region. If *Mark*=2, denotes that there is no circular connected region in D_o, and the circular connected region in the iris image I needs to be found by Hough transform. In order to facilitate discussion and description, we define the function $[C_i, R_i]$=GetCirclePara(D_0,*Mark*) of extracting the parameters of the connected region, which is described as follows:

- *Function* 3. $[C_i, R_i]$=GetCirclePara (I, D_0,*Mark*) Input parameters: I is the iris image, D_0 is the binary image, and *Mark* is the marker which whether there is a circular connected region in D_0.
- Output parameters: D_0 is the image produced by the function, and *Mark* is the maker whether there is a circular connected region in D_0. C_i and R_i are the center and the radius of the circular connected region respectively, namely the center and the radius of the iris inner boundary.
- *Step* 1. If *Mark*=1, for the circular connected region S_0 in D_0, the following steps are performed:

  a) The centroid coordinates *Center* (x_o,y_o) of the connected region are derived.
  b) The major axis *Ma* of the connected region is calculated;
  c) The radius R_e of a circle with the same area as the connected region is computed:

$$\pi R_e^2 = A_0 \qquad (14)$$

  d) The radius *Radius* of the connected region is worked out:

$$Radius = \frac{0.5 * Ma + R_e}{2} \qquad (15)$$

Return C_i=*Center* and R_i=*Radius*, and the function ends.

- *Step* 2. If *Mark*=2, for the iris image I, the following steps are performed:

  a) Initialization: the circular region mean filter *Gs* with the size of 3 is created, and the image scaling factor *SF*=4.
  b) *Gs* is used to filter the iris image I to obtain the image F.
  c) The filtered image F is reduced to 1/*SF* to obtain the image F'.
  d) Canny operator is used for edge detection of the image F' to obtain the binary edge image E;
  e) The edges connected to the boundary of E in the 8-neighborhood connection, and then those whose lengths are less than 20 pixels in E, are deleted to obtain the image E_d.
  f) The size of the image E_d is *Rows*×*Cols*, let R_{max}=min(*Rows*,*Cols*), and the maximum radius of a circle explored by Hough transform in E_d is limited according to R_{max}.
  g) Hough transform is used to find a circle with the radius being $[1,R_{max}/(2*SF]$ in E_d to get the circle center *Center* and the radius *Radius*.
  h) Return C_i=*Center* and R_i=*Radius*, and the function ends.

4.4. Obtaining the Parameters of the Iris Inner Boundary

From the statement above, a method for extracting the iris Inner Boundary based on morphology operations with Multi-structural Elements is described as follows:

- *Step* 1. The iris image I is preprocessed, namely, [D,m]=PreImage(I,2000);

- *Step* 2. The circular connected region is determined in D, that is, the function [D_0,*Mark*]=DCGF(D) is called;

- *Step* 3. The parameters of the circular connected region are extracted, i.e., the function $[C_i,R_i]$=GetCirclePara(I,D_0,*Mark*) is called to get the center and the radius of the iris inner boundary.

According to the method stated above, three images are selected as experimental images, including Image S1138R05 in the Casia-V3.0-Interval, Image S2161R09 in the Casia-V3.0-Lamp, and Image S3202R02 in the Casia-V3.0-Twins, respectively, as illustrated in Figure 3. The iris inner boundaries of the above images are located by IBME, and the results are shown in Figure 4. From Figure 4, all the pupils in the three images can be accurately located and the centers and the radiuses of the pupils are obtained. The experimental results show that, the center of Figure 3-a) is (154.7921,147.2137) and the radius is 49.6967, those of Figure 3-b) (351.0790, 249.4517) and 33.9583, and those of Figure 3-c) (303.9323, 212.6939) and 39.0961.

a) Image S1138R05.	b) Image S2161R09.	c) Image S3202R02.

Figure 3. The Iris images.

a) Image S1138R05.	b) Image S2161R09.	c) Image S3202R02.
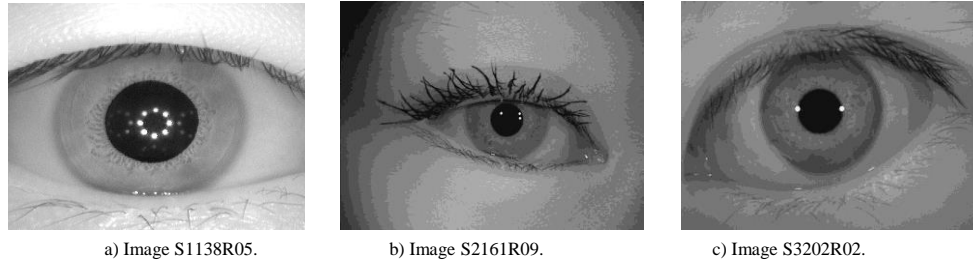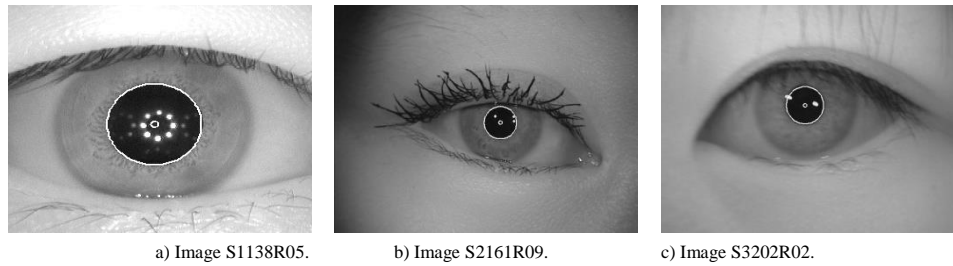
Figure 4. Location of the iris inner boundaries of the three images in Figure 3.

5. Location of the Iris Outer Boundary

Because the center of the iris outer boundary may be deviated from that of the iris inner boundary in the image, the latter can only be reckoned as the result of coarse location of the former. So the center $C_i(x_i,y_i)$ and the radius R_i of the iris inner boundary are referred to as the initial values for the location of the iris outer boundary. Because the gray scale change of the iris outer boundary is not obvious compared with that of its adjacent pixels, if the method for locating the iris inner boundary is performed on dealing with the iris outer boundary, the exact iris outer boundary cannot be extracted. In this paper, a method for locating iris Outer Boundary based on Annular region and Hough transform is introduced.

First of all, the iris image I is filtered by the circular region mean filter, and the filtered image F is produced. In order to speed up Hough transform to find the circle, we reduce F to $1/SF$ with the scaling factor $SF=4$, and the scaling image F' is obtained. Then Canny operator is used for edge detection of F' to get the binary edge image E, and the edges connected to the boundary of E are removed in the 8-neighborhood connection to get the image E_d. Finally, the annular region with the center at $C_i(x_i,y_i)/SF$ and the range $[R_i+30,R_i*3.0]/SF$ of the radius is intercepted in the image E_d to obtain the annular image E_r, where Hough transform is employed to explore the circle, and the center coordinate and the radius R_o of the iris outer boundary are extracted. As expounded above, OBAH is described in details as follows:

- *Step* 1. Initialization: the circular region mean filter Gs with the size of 3 is created, and the image scaling factor $SF=4$.
- *Step* 2. The iris image I is filtered by Gs to get filtered image F.
- *Step* 3. The image F is scaled by $1/SF$ to get the image F'.
- *Step* 4. Edge detection is performed on F' by Canny operator to obtain binary edge image E;
- *Step* 5. The edges connected to the boundary in the 8-neighborhood connection are removed in E to get the image E_d.
- *Step* 6. The annular region with the center at $C_i(x_i,y_i)/SF$ and the range $[R_i+30,R_i*3.0]/SF$ of the radius is intercepted in the image E_d to obtain the annular image E_r.
- *Step* 7. Hough transform is used to find a circle in E_r, and the range of exploring the radius is $[R_i+30,R_i*3.0]/SF$.
- *Step* 8. According to the center coordinate $C_H(x_H,y_H)$ and the radius R_H obtained by Hough transform, the center coordinates and the radius of the iris outer boundary are derived as $C_o(x_o,y_o)= C_H(x_H,y_H)*SF$ and $R_o=R_H*SF$ respectively.

According to the above method, the iris outer boundaries of the three images in Figure 3 are located, as shown in Figure 5. From Figure 5, we can know that, the centers and the radiuses of the iris outer boundaries are accurately obtained in all the three images. The center and the radius are (152,144) and 108 In Figure 3-a) respectively, those (352,248) and 88 in Figure 3-b), and those (304,216) and 108 in Figure 3-c). Also, we find that the centers of the iris inner and outer boundaries do not coincide completely.

a) Image S1138R05.   b) Image S2161R09.   c) Image S3202R02.
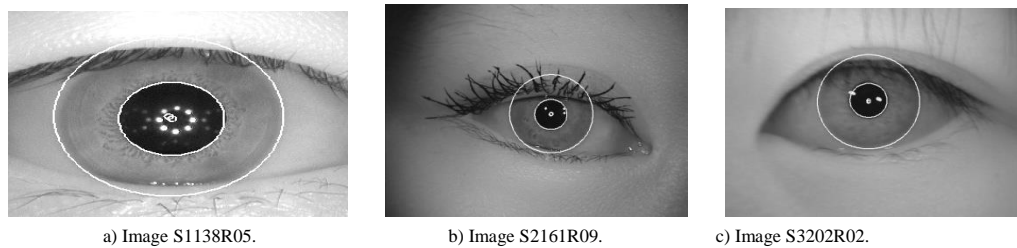
Figure 5. Location of the outer boundaries of the three images in Figure 3.

6. Experimental Results and Discussions

In this paper, all the experimental images are carried out in MATLAB 7.11(R2010b) on PC with an Intel Core(TM) i3-4130 ® 3.4GHz and 4GB RAM, running 64-bit Windows 7. In order to verify the effectiveness of this proposed method, the performance comparison is tested between this proposed method and Ma *et al.* method [14], which mainly covers two indexes of Location Accuracy Rate (LAR) and the Average Running Time (ART). In this section, the experimental iris images are taken from three databases including Casia-V3.0-Interval, Casia-V3.0-Lamp and Casia-V3.0-Twins, founded by the Institute of Automation, Chinese academy of sciences. One hundred iris images are randomly chosen from each database as the experimental images. It is worth noting that, the images from CASIA-V3.0-Interval are the size of 320×240, but those from CASIA-V3.0-Lamp and CASIA-V3.0-Twins are 640×480 pixels, and the gray level of all the images is 256 . The experimental results from this proposed method, Ma *et al.* [14] method and Daugman [7] method are demonstrated in Table 1, and the implementation results of the various values *Mark* of locating the iris inner boundary by this proposed method are shown in Table 2.

It can be seen from Table 1, for the location accuracy of one hundred images randomly selected from casia-V3.0-Interval, LAR of this proposed method is highest than those of Ma *et al* [14] method and Daugman method [7] in locating the iris inner and outer boundaries. As for ART of locating the iris inner boundary, this proposed method is lowest than Ma *et al.* [14] method and Daugman [7] method, which is 1.3466 and 0.5563 times faster respectively and has an obvious advantage. When locating the iris outer boundary, this proposed method is 0.0644 and 0.1884 seconds faster than Ma *et al.* [14] method and Daugman [7] method respectively. As a whole, this proposed method is 0.3476 and 0.3054 seconds faster than Ma *et al.* [14] method and Daugman [7] method respectively, and the speed is increased by 49.43% and 46.20% respectively.

From Table 1, for one hundred images randomly selected from CASIA-V3.0-Lamp, LAR of this proposed method is significantly highest than those of Ma *et al.* [14] method [14] and Daugman [7] method in locating the iris inner and outer boundaries. In terms of ART of the iris inter boundary location, this proposed method is far lowest than Ma *et al.* [14] method and Daugman [7] method, which is 3.7129 and 0.3285 times faster respectively and has an advantage. For the iris outer boundary, this proposed method is 0.1799 and 0.6430 seconds faster than Ma *et al.* [14] and Daugman [7] method respectively. Therefore, the overall ART of this method is 2.0163 and 0.8055 seconds faster than that Ma *et al.* [14] method and Daugman [7] method respectively, and the speed is increased by 2.7104 and 1.0828 times respectively.

We also can know from Table 1, for one hundred images randomly selected from CASIA-V3.0-Twins, the performance of this proposed method has obvious advantages compared with those of Ma *et al.* [14] method and Daugman [7] method. LAR of this proposed method is highest than those of Ma *et al.* [14] method and Daugman [7] method in both the iris inner and outer boundary locations. Taking into consideration of ART of locating the iris inner boundary, this proposed method is still lowest than Ma *et al.* [14] method and Daugman [7] method, which is 3.2839 and 0.5322 times faster respectively and possesses a compelling advantage. For locating the iris outer boundary, this proposed method is 0.0583 and 0.5723 seconds faster than Ma *et al.* [14] method and Daugman [7] method respectively. From an overall perspective of ART, this proposed method is 1.5657 and 0.8167 seconds faster than that of Ma *et al.* [14] method and Daugman [7] method respectively, and the speed is increased by 66.13% and 50.46% respectively.

From the above analysis, it can be seen that, this proposed method has an overwhelming advantage over the Ma *et al.* [14] method and Daugman [7] method in terms of ART of the iris inter boundary location. Especially, the bigger the image is, the more

obvious the advantage is. When locating the iris outer boundary, compared with Ma *et al*. [14] method and Daugman [7] method, ART of this proposed method has a slight advantage. On the whole, this proposed method has higher locating accuracy and lower locating time than Ma *et al*. [14] method and Daugman [7] method.

From Table 2, the more time-consuming location with *Mark*=2 does not occur in the three image databases. In fact, all the images are performed only by the location with *Mark*=1 and the center and the radius of the iris inner boundary are obtained. In this case of *Mark*=2, the locating speed is very fast and the time consumption is very low. Therefore, the iris inner boundary locations with the various values *Mark* in Table 2 are consistent with the fact that the iris inner boundary locating efficiency of this proposed method is much better than that of Ma *et al*. [14] method in Table 1.

Table 1. Comparison of the location accuracy rate and the running time.

Image database	Location method	ART(S)			LAR(%)		
		Inner boundary	Outer boundary	Overall	Inner boundary	Outer boundary	Overall
Interval	This proposed Method	0.2103	0.1453	0.3556	96%	95%	95%
	Ma *et al*. Method [14]	0.4935	0.2097	0.7032	92%	93%	92%
	Daugman method [7]	0.3273	0.3337	0.6610	92%	92%	92%
Lamp	This proposed Method	0.4946	0.2493	0.7439	97%	96%	96%
	Ma *et al*. Method [14]	2.3310	0.4292	2.7602	92%	92%	92%
	Daugman method [7]	0.6571	0.8923	1.5494	93%	93%	93%
Twins	This proposed Method	0.4590	0.3429	0.8018	97%	96%	96%
	Ma *et al*. Method [14]	1.9663	0.4012	2.3675	91%	92%	91%
	Daugman method [7]	0.7033	0.9152	1.6185	92%	93%	92%

Table 2. Comparison of the iris inner boundary locations with the various values Mark.

Image database	*Mark*=1		*Mark*=2	
	Number of images	ART(S)	Number of images	ART(S)
Interval	100	0.2103	0	0
Lamp	100	0.4946	0	0
Twins	100	0.4590	0	0

The accurate location method requires that the iris inner and outer boundaries obtained are consistent with the actual boundaries, in other words, there is no boundary deviation, no over-segmentation or under-segmentation. Because of the space limitation, this paper only uses four groups of the located images from each database to be exhibited in Figures 6 to 14. where Figures 6, 7, and 8 are the results of four groups of one hundred images from CASIA-V3.0-Interval, Figures 9, 10, and 11 are the results of four groups of one hundred images from CASIA-V3.0-Lamp, and Figures 12, 13, and 14 are the results of four groups of one hundred images from CASIA-V3.0-Twins, respectively after being located by Ma *et al*. [14] method, Daugman [7] method and this proposed method.

a) Interval 1.   b) Interval 2.   c) Interval 3.   d) Interval 4.
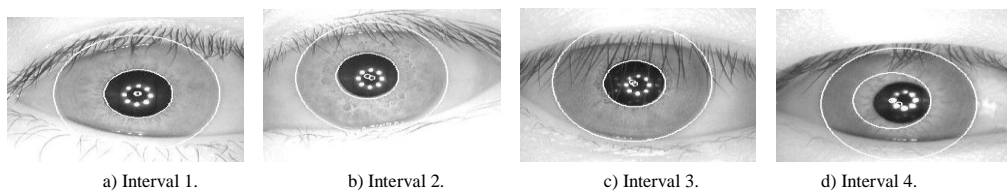
Figure 6. Results of four groups of one hundred images from CASIA-V3.0-Interval after being located by Ma method [14].

a) Interval 1.   b) Interval 2.   c) Interval 3.   d) Interval 4.
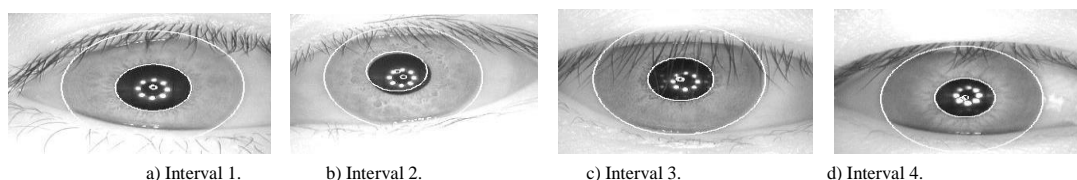
Figure 7. Results of four groups of one hundred images from CASIA-V3.0-Interval after being located by Daugman method [7].

a) Interval 1.   b) Interval 2.   c) Interval 3.   d) Interval 4.
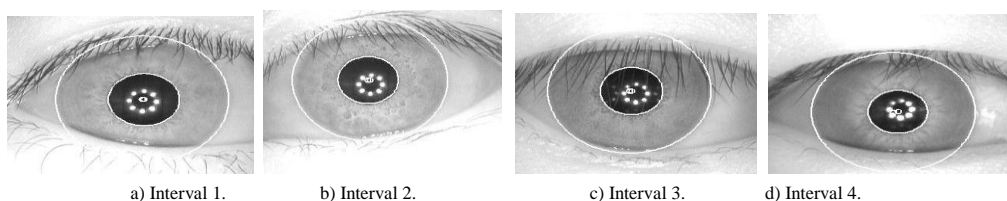
Figure 8. Results of four groups of one hundred iris images from CASIA-V3.0-Interval after being located by this proposed method.

a) Lamp 1.   b) Lamp 2.   c) Lamp 3.   d) Lamp 4.
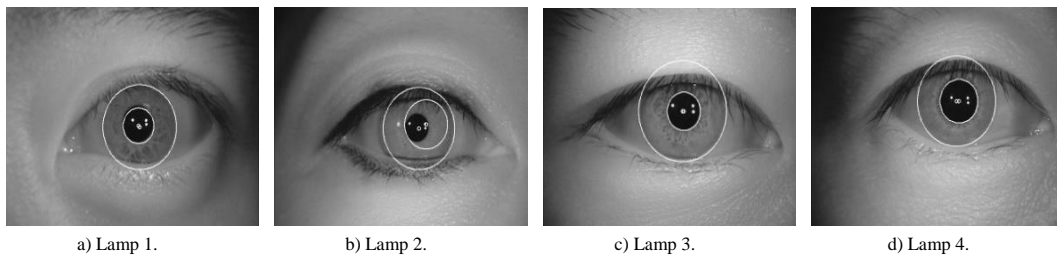
Figure 9. Results of four groups of one hundred iris images from CASIA-V3.0-Lamp after being located by Ma method [14].

a) Lamp 1.   b) Lamp 2.   c) Lamp 3.   d) Lamp 4.
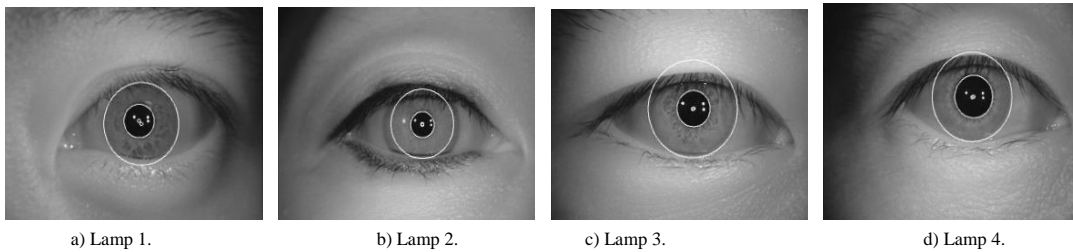
Figure 10. Results of four groups of one hundred iris images from CASIA-V3.0-Lamp after being located by Daugman method [7].

a) Lamp 1.   b) Lamp 2.   c) Lamp 3.   d) Lamp 4.
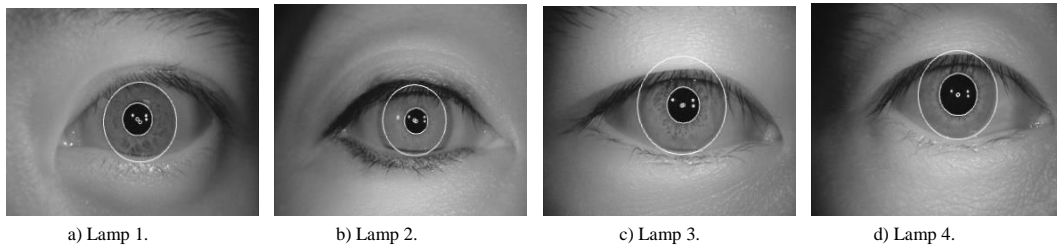
Figure 11. Results of four groups of one hundred iris images from CASIA-V3.0-Lamp after being located by this proposed method.

a) Twins 1.   b) Twins 2.   c) Twins 3.   d) Twins 4.
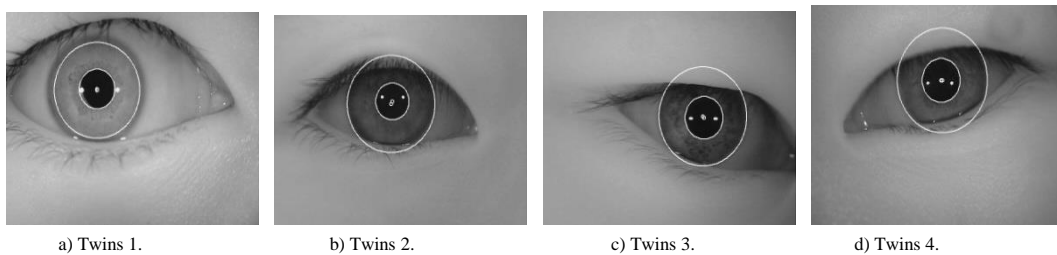
Figure 12. Results of four groups of one hundred iris images from CASIA-V3.0-Twins after being located by Ma method [14].

a) Twins 1.   b) Twins 2.   c) Twins 3.   d) Twins 4.
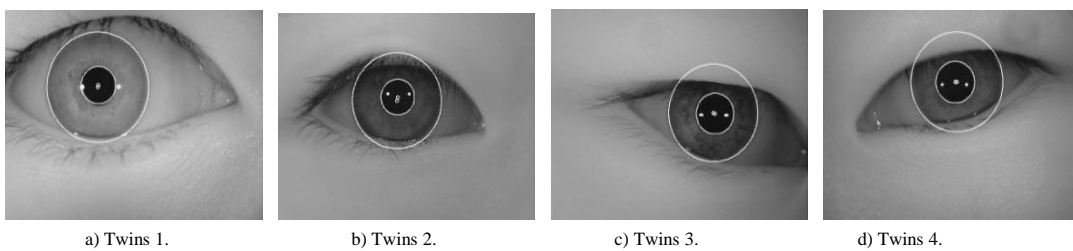
Figure 13. Results of four groups of one hundred iris images from CASIA-V3.0-Twins after being located by Daugman method [7].

a) Twins 1.   b) Twins 2.   c) Twins 3.   d) Twins 4.
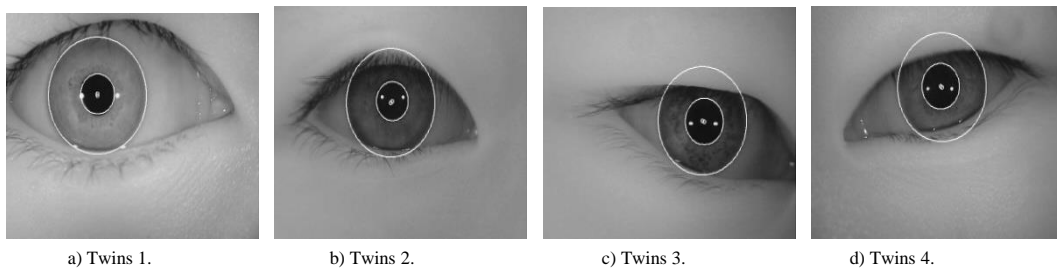
Figure 14. Results of four groups of one hundred iris images from CASIA-V3.0-Twins after being located by this proposed method.

For most of the images, the three methods acquire good locating effect under different conditions. But it's important to note that, that since the pupil in the iris image is not necessarily a standard circle, there exists

a slight difference in the locating results. To be specific, Ma *et al.* [14] method uses Hough transform to obtain the iris inner and outer boundary parameters. Although Hough transform has a high accuracy in exploring the center and the radius, it has a high time complexity, so it is necessary to zoom out the image and reduce the amount of data before Hough transform to improve the efficiency of searching for a circular connected region. Besides, small objects such as eyelids and eyelashes will have a greater influence on the iris inner boundary location. Daugman method [7] uses calculus operators to calculate the maximum edge gradient to complete iris edge positioning. This method is accurate for most images, but due to complex differential and integral operations, the locating speed is slow, and the locating efficiency is low when the image resolution is large. In addition, for some images with strong edge interference, spot and eyelash have a great influence on the location result, and the result of edge location will fall into the local minimum problem. In this paper, the affect of small objects is weakened by mathematical morphology, and the circular connected region is determined according to the region geometric features. Then, the center and the radius are extracted from the circular connected region, and the location of the iris inner boundary is finished. For the location of the iris outer boundary, the circular region mean filter can effectively avoid the interference of upper eyelid, eyelash and spot. In addition, we find that Figures 6-d) and 9-b) obtained by Ma *et al.* [14] method and Figure 7-b) obtained by Daugman [7] method, fail to locate the iris inner boundaries, while in Figures 8-b), 8-d) and 11-b), this proposed method can successfully locate the iris inner boundaries. It's worth noting that, however, although the location result in Figure 11-b) is successful, the radius of the iris outer boundary is slightly smaller. It can be seen from Figure 12-a) that, Ma *et al.* [14] method can successfully locate the iris inner and outer boundaries, but the radius of the iris outer boundary is slightly smaller. The main reason for the failure of Ma *et al.* [14] method is that the location accuracy of Hough transform is affected by the searching radius, but this proposed method obtains relevant parameters of the connected region through performing mathematical morphology operations on the iris image, and achieves good results without preset initial value.

The main reasons for the good location performance of this proposed method are as follows:

1. In the course of pre-processing by the gray stretch transform, the iris image is shrunk, which significantly reduces the amount of K-means clustering data. When K-means clustering, ITM is used to generate the initial clustering center, which effectively shortens the convergence time of the algorithm.

2. When there are multiple connected regions in the binary image, the connected region with the largest area is retained, which reduces the interference of other connected ones, shortens the time to obtain the pupil region, and improves the accuracy of locating the iris inner boundary.

3. After dealing with preprocess, each image retains only one connected region in line with the circular geometrical features, then the center and the radius of the iris inner boundary can be directly obtained by calculating the centroid, the major axis, minor axis and the radius of a circle with the same area as the connected region, which greatly shorten the time for iris inner boundary parameters.

4. The accuracy location of the iris inner boundary lays a solid foundation for locating the iris outer boundary. When the iris outer boundary location, although also using Hough transform, but reducing the iris image and cropping the annular region make the range of the searching radius of Hough transform be narrowed, which significantly reduces the amount of data and improves the locating speed.

7. Conclusions

Iris location is one of the hot topics in image processing for a long time. In this paper, an improved iris localization method. When locating the iris inner boundary, a method for extracting the iris inner boundary based on morphology operations with multi-structural elements is explained by preprocessing the iris image and exploring the circular connected region. When locating the iris outer boundary, a method for locating iris outer boundary based on annular region and Hough transform is introduced by reducing the iris image and intercepting the annular region within a certain range. Meanwhile, this paper also analyzes and compares the locating effect of Ma *et al.* [14] method and Daugman [7] method. The experimental results reveal that the location accuracy rate of this proposed method is at least 95% and the average running time is increased by 46.2% even higher. Therefore, this proposed method is effective and reliable, with strong robustness and more flexible.

Acknowledgements

Technology Innovative Research Team in Higher Educational Institutions of Hunan Province.

References

[1] Alvarez-Betancourt Y. and Garcia-Silvente M., "A Key Points-Based Feature Extraction Method for Iris Recognition Under Variable Image Quality Conditions," *Knowledge Based Systems*, vol. 92, no. (C), pp. 169-182, 2016.

[2] Arunachalamand M. and Amuthan K., "Finger Knuckle Print Recognition using MMDA with Fuzzy Vault," *International Arab Journal of Information Technology,* vol. 17, no. 4, pp. 554-561, 2020.

[3] Boles W., "A Security System Based on Human Iris Identification Using Wavelet Transform," *in Proceedings of the 1ˢᵗ International Conference on Knowledge-Based Intelligent Electronic Systems*, Adelaide, pp. 533-541, 1997.

[4] Bowyer K., Hollingsworth K., and Flynn P., "Image Understanding for Iris Biometrics: A Survey," *Computer Vision and Image Understanding*, vol. 110, no. 2, pp. 281-307, 2008.

[5] Chang Y., Shih T., Li Y., and Kumara W., "Effectiveness Evaluation of Iris Segmentation By Using Geodesic Active Contour (GAC)," *The Journal of Supercomputing*, vol. 76, no. 3, pp. 1628-1641, 2020.

[6] Daugman J., "Statistical Richness of Visual Phase Information: Update on Recognizing Persons by Iris Patterns," *International Journal of Computer Vision*, vol. 45, no. 1, pp. 25-38, 2001.

[7] Daugman J., "The Importance of Being Random: Statistical Principles of Iris Recognition," *Pattern Recognition*, vol. 36, no. 2, pp. 279-291, 2003.

[8] Doan H. and Nguyen D., "A Method for Finding the Appropriate Number of Clusters," *The International Arab Journal of Information Technology*, vol. 15, no. 4, pp. 675-682, 2018.

[9] Efimov Y., Leonov V., Odinokikh G., Solomatin I., "Finding the Iris Using Convolutional Neural Networks," *Journal of Computer and Systems Sciences International*, vol. 60, no. 1, pp.108-117, 2021.

[10] Jan F., Min-Allah N., Agha S., Usman I., and Khan I., "A Robust Iris Localization Scheme for The Iris Recognition," *Multimedia Tools and Applications*, vol. 80, no. 18, pp. 4579-4605, 2021.

[11] Kadir K., Gao H., Payne A., Soraghan J., and Berry C., "LV Wall Segmentation Using The Variational Level Set Method (LSM) with Additional Shape Constraint for Oedema Quantification," *Physics in Medicine and Biology*, vol. 57, no. 19, pp. 6007-6023, 2012.

[12] Li P., Liu X., Xiao L., and Song Q., "Robust and Accurate Iris Segmentation in Very Noisy Iris Images," *Image and Vision Computing*, vol. 28, no. 2, pp. 246-253, 2010.

[13] Lin Y., Hsieh T., Huang J., Yang C., Shen V., and Bui H., "Fast Iris Localization Using Haar-Like Features and Adaboost Algorithm," *Multimedia Tools and Applications*, vol. 79, no. 12, pp. 34339-34362, 2020.

[14] Ma L., Tan T., Wang Y., and Zhang D., "Efficient Iris Recognition by Characterizing Key Local Variations," *IEEE Transactions Image Process*, vol. 13, no. 6, pp. 739-750, 2004.

[15] Schuckers S., Schmid N., Abhyankar A., Dorairaj V., Boyce C., and Hornak L., "On Techniques for Angle Compensation in Nonideal Iris Recognition," *IEEE Transactions on Systems, Man, and Cybernetics, Part B (Cybernetics)*, vol. 37, no. 5, pp. 1176-1190, 2007.

[16] Sudha N., Puhan N., Xia H., and Jiang X., "Iris Recognition on Edge Maps," *IET Computer Vision*, vol. 3, no. 1, pp. 1-7, 2009.

[17] Tan T., He Z., and Sun Z., "Efficient and Robust Segmentation of Noisy Iris Images for Non-Cooperative Iris Recognition," *Image and Vision Computing*, vol. 28, no. 2, pp. 223-230, 2010.

[18] Zheng Z., Yang J., and Yang L., "A Robust Method for Eye Features Extraction on Color Image," *Pattern Recognition Letters*, vol. 26, no. 14, pp. 2252-2261, 2005.

Meisen Pan was born in 1972 and graduated from Hunan Normal University, China, in 1995. He received the M.S. degree from Huazhong University of Science and Technology, China, in 2005. He obtained the Ph.D. degree from Central South University, China, in 2011. Currently, he is a professor in the College of computer and electrical engineering at Hunan University of Arts and Science. He has published more than 40 papers on journals and conferences. His research interests include biomedical image processing, information fusion and software engineering.

Qi Xiong was born in 1971 and received his M.S. degree from Huazh ong University of Science and Techn ology, China, in 2005, Currently, he is a senior engineer in the College of computer and electrical engineering at Hunan University of Arts and Science. He has published more than 10 papers in journals and conferences. His re search interests include Biometric recognition, informat ion fusion, and software engineering.